Available online at www.sciencedirect.com
SCIENCE DIRECT
Polymer 47 (2006) 2357–2368
polymer
www.elsevier.com/locate/polymer

Effect of the particle size on the viscoelastic properties of filled polyethylene

Maged A. Osman *, Ayman Atallah [1]

Department of Materials, Institute of Polymers, Wolfgang-Pauli-strasse 10, ETH Zurich, 8093 Zurich, Switzerland

Received 2 December 2005; received in revised form 21 January 2006; accepted 26 January 2006
Available online 20 February 2006

Abstract

Composites of surface treated and non-treated colloidal calcium carbonate and high-density polyethylene with different filler loading were prepared. Their viscoelastic properties were studied by dynamic strain sweep and small-amplitude oscillatory shear, and compared to those of the corresponding composites of micron-sized calcite. The specific surface area of the filler enormously increases as the average particle diameter becomes smaller than 600 nm, leading to a strong tendency to agglomeration (soft flocks) and aggregation (hard clusters that need attrition to be disintegrated). In nanocomposites, more and stronger filler clusters are formed than in microcomposites due to the large contact area between the particles. The clusters have different shapes and maximum packing than the nearly spherical primary particles, thus enhance the moduli and viscosity of the composites. The obtained results indicate that the higher moduli and viscosity of the nanocomposites is not a direct consequence of the particle size but is due to the presence of more agglomerates and aggregates. Clusters that are local structures and do not represent a space-filling filler network enhance the moduli in the low frequency region more than at high frequencies and increase the storage more than the loss modulus. The presence of strong local structures in the nanocomposites leads to weak log moduli–log frequency dependence in the low frequency (terminal) region. Polymer adsorption on the particles' surface results in a transient filler–polymer network and slow dynamics of the bound polymer, which contribute to the moduli of the complex fluid. The sum of all these factors leads to gradual increase in moduli and to a shift of the crossover frequency to lower values. Above a certain filler volume fraction, the composite responds as a viscoelastic solid (storage modulus > loss modulus over the whole frequency range and both moduli are frequency independent in the terminal zone of the log–log plot).

Keywords: Polyethylene; Calcium carbonate; Particle size

1. Introduction

Polyethylene (PE) is widely exploited in different applications and is often compounded with minerals to adapt its properties to the requirements of a specific application. One of the prominent goals of filler addition is mechanical reinforcement [1,2]. Calcium carbonate is the most abundant mineral and exists in different crystal forms but calcite is that most widely found, therefore PE-calcite composites are of considerable industrial interest. The filler particle diameter varies from several microns to few nanometers depending on the production method. In PE composites, solid particles often build agglomerates (soft flocks) or aggregates (hard clusters that need attrition to be disintegrated), depending on their surface area, surface energy, filler–polymer interactions and compounding conditions. To reduce the calcite high surface energy and the interparticle interactions, its surface is often coated with a variety of surface modifiers; however, stearic acid is that mostly used [3]. As previously pointed out, studying the influence of solid inclusions on the properties of the polymer melt has the advantage of avoiding additional variables arising from PE crystallization in the solid state and gives insight into the mechanism of polymer reinforcement [4].

Hydrodynamic and micromechanics models predict that the mechanical and viscoelastic properties of polymer composites are particle size independent [5–9]. However, contradictory results exist in the literature and the effect of submicron spherical particles on the dynamic mechanical properties and the viscoelasticity is controversial [10,11]. Van der Werff and de Kruif [12] found that the viscosity of colloidal silica particle dispersions is particle size independent, confirming the models' predictions, while other authors reported strong influence of the particle size on the viscosity and moduli of polymer melts

* Corresponding author. Tel.: +41 44 6324653; fax: +41 44 6321096.
E-mail address: mosman@mat.ethz.ch (M.A. Osman).
[1] Present address: Physics Department, Faculty of Science, Beni Suef University, Beni Suef, Egypt.

0032-3861/$ - see front matter © 2006 Elsevier Ltd. All rights reserved.
doi:10.1016/j.polymer.2006.01.085

[13–15]. Poslinski et al. [16] reported that, in the same matrix, large glass spheres ($d \geq 10$ μm) did not show evidence of a yield stress up to 60 vol%, while small ceramic particles ($d = 1$ μm) exhibited a yield stress at 50 vol% concentration. In contrast to composites of micron-sized fillers, large increases in viscosity and linear viscoelastic moduli as well as the presence of a terminal plateau in the log–log plots of $G'(\omega)$ and $G''(\omega)$ have been observed in nanocomposites at low filler loading [13–15,17–22]. Li and Masuda [14] attributed the differences in properties of both types of composites to the formation of 'agglomerated and network structures'. It has also been reported that the filler volume fraction at which a terminal plateau is observed depends on the interfacial tension and the stiffness of the particles beside the particle size [15,19,20]. As the particles surface energy is decreased due to surface treatment of the filler, the viscosity and dynamic moduli decrease [13,19,23]. Similar observations were made for nano-particle dispersions and filled elastomers, and fractal structures were suggested [11,24–28]. The observed low-frequency plateau (solid-like response) in the moduli-frequency log–log plots has been often attributed to the presence of a particle network and percolation limits as low as 0.02 were postulated for fillers with spherical primary particles [11,21,22,27,29]. However, the viscosity percolation limit is generally larger than the geometrical percolation threshold and the three-dimensional geometrical percolation threshold of monodisperse spheres has been calculated to be 0.289 (the threshold for polydisperse spheres is probably higher) [30–32]. A filler network (percolated inclusions) can also be expected to lead to an elastic response ($G' \gg G''$ and log frequency independent log moduli) over the entire experimentally accessible frequency range [33].

Other authors attributed the pseudo-solid response in the low frequency zone to polymer adsorption on the filler surface that provides additional localized junctions, resulting in a transient network or entrapped entanglements [25,34,35]. However, usually entanglements get entrapped between permanent junctions such as chemical cross-links. Polymer adsorption can also lead to a higher effective filler volume fraction, whose magnitude depends on the surface area of the inclusions and the strength of the filler–polymer interactions (layer thickness) [36]. The dynamics of the adsorbed (bound) polymer is also expected to be different from that of the bulk polymer, leading to an increase in viscosity and moduli [37,38].

In the present study, nano-sized calcium carbonate particles ($d \approx 80$ nm), surface treated (stearic acid) and non-treated, were compounded with linear high-density polyethylene (HDPE) at different filler loading. The dynamic moduli and viscosity of the composites were compared to those of the corresponding microcomposites, in order to get insight into the effect of particle size on the dynamic mechanical and viscoelastic properties of polymer melts.

2. Experimental

2.1. Materials

The HDPE used is Hostalen GF 9055F, supplied by Basell (Mainz, Germany). It had a density of 0.954 g/mL (23 °C), a melt flow index of 0.5 g/10 min (2.16 kg at 190 °C) and a zero shear viscosity of 32 kPa s at 170 °C. Precipitated (ppt) calcium carbonate powders U1 and U1S2 (stearic acid surface treated) with an average diameter of ca. 80 nm and BET specific surface area (SSA) = 20 m^2/g (supplier data) were courtesy of Solvay (Ebensee, Austria). The coated organic layer in U1S2 was found by thermogravimetric analysis (TGA, 50–490 °C) to consist 3.1% of the filler's weight. The properties of the micron-sized calcite (VP 1018) and its composites, used for comparison, have been previously described [3,4,39].

2.2. Sample preparation

Composites containing different inorganic volume fractions of the filler with and without surface coating were prepared in a twin-blade kneader 'Plasti-Corder W 50 EH' (Brabender, Duisburg, Germany) equipped with a 60 mL bowl and counter-rotating blades. Above 13 vol% U1 or 25 vol% U1S2, it was difficult to homogeneously distribute the filler in the polymer matrix. The filler volume fraction (ϕ) was calculated using the densities of calcite (corrected in U1S2) and HDPE, which gives the volume of the filler as if it was in a compact state or if the particles were fully dispersed. In presence of clusters, the effective filler volume fraction becomes larger due to the presence of interstices even if the polymer is not entrapped in these cavities as in HDPE–calcite composites [39]. However, in case of non-wetting polymers the increase in ϕ is relatively small as long as the volume of the interstices is only given by the particles geometry and the number of clusters is limited [40]. The compounding conditions were chosen to minimize polymer degradation (verified by comparing the viscosity of kneaded and pristine neat polymer) and achieve optimal homogenization of the filler. The polymer pellets were molten at 150 °C and the required amount of filler was gradually added within 15–20 min at 40 rpm. The speed was then increased to 60 rpm and the mixture homogenized for further 8 min. The amount of material was chosen to completely fill the bowl and avoid incorporation of air that promotes polymer degradation during compounding.

The compound was compression molded to 1.5 mm thick plaques in a brass frame between two aluminum plates at 180 °C. The compression molding process was carried out under reduced gas pressure (0.01 mbar) in a brass chamber. The composite was carefully degassed before and during molding to ensure the absence of micro-voids and the mold was left to cool slowly under pressure. Discs 20 mm in diameter, whose edges were brows free, were stamped out of the plaques for the rheological measurements.

2.3. Scanning electron microscopy (SEM)

To study the morphology of the composites, a cryo-fractured surface was etched with a cold oxygen plasma for 2 min, sputter coated with 3 nm of Pt and observed in a Hitachi S-900 'in-lens' field emission scanning electron microscope (FESEM) at 10 kV accelerating voltage. Samples of the filler powder were deposited on a carbon coated EM-grid from a

sonicated dilute alcoholic suspension, sputter coated with Pt and examined as described above.

2.4. Rheological testing

The rheological properties were measured using a stress- and strain-controlled rheometer (MCR 300-Physica, Stuttgart, Germany) equipped with an electrically heated thermostating unit (TEK 350-CF). The experiments were carried out with a cone–plate geometry ($d=50$ mm, angle $=4°$, truncated 50 μm) at 170 °C under nitrogen to obtain a uniform stress field. All samples ($d=20$ mm) were dried at 70 °C under reduced pressure over night. They were allowed to fully relax after squeezing in the rheometer (monitored by measuring the normal force) before starting the measurement. The strain-controlled experiments included dynamic strain amplitude γ_0 sweep (logarithmically increasing from 0.04 to 100%) at a fixed angular frequency $\omega=1$ rad/s, and small-amplitude ($\gamma_0=$ 0.05%) oscillatory shear measurements, in which ω was logarithmically increased from 0.02 to 600 rad/s. Each sample underwent the following tests in sequence and in this order: frequency sweep (FS), amplitude sweep (AS) followed by a relaxation period of 0.5–1 h (depending on the filler concentration), frequency sweep and an amplitude sweep. The sample relaxation was monitored by observing the decrease in shear rate by time. For the frequency sweeps, a low amplitude was chosen to ensure that the dynamic moduli are measured in the linear viscoelastic regime with the same amplitude for all filler concentrations. The average of three measurements for each sample is reported. Time sweeps showed that the samples were thermally stable (constant rheological response) over the time scale of the experiment.

3. Results and discussion

A SEM micrograph of the filler powder U1 (precipitated calcium carbonate) is given in Fig. 1, showing that the nanoparticles are nearly spherical and some of them seem to be fused together. Qualitatively, their particle size distribution is narrower than that of the micron-sized milled calcite VP 1018 [3]. The surface treated (stearic acid) filler U1S2 has the same morphology and SSA.

Repetitive dynamic strain amplitude sweeps, in which the specimen was allowed to relax after each run, were carried out with a fixed $\omega=1$ rad/s. The inorganic volume fraction was varied in the range 0–13% for U1 and 0–25% for U1S2. The complex viscosity $|\eta^*|$, measured in two consecutive runs is plotted as a function of γ_0 in Fig. 2 (for clarity only the high concentrations are shown). A large decrease in the zero complex viscosity $|\eta^*|$ can be observed in the second run, whereas there is practically no difference in $|\eta^*|$ at $\gamma_0=100\%$. The difference in $|\eta_0^*|$ between the two runs decreases with declining ϕ and with surface treatment, pointing out that the viscosity reduction is due to the disintegration of agglomerates, whose number and size increase with increasing filler loading as was observed in case of the non-colloidal calcite composites [4,39]. The viscoelastic linear regime is also smaller in the first run than in the second,

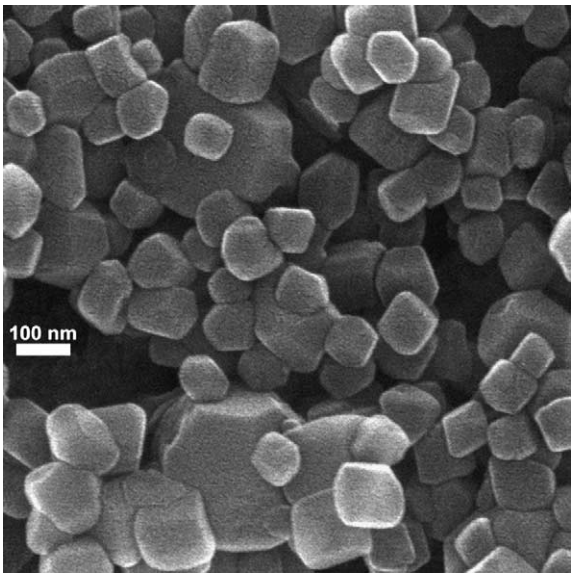

Fig. 1. SEM micrograph of the non-treated colloidal $CaCO_3$ (U1) powder.

especially at high ϕ, i.e. γ_0 corresponding to the onset of the nonlinear viscoelasticity increases as a result of shearing in the first AS. That is, clusters increase the viscosity and enhance the viscoelastic nonlinearity. The presence of agglomerates and aggregates in the compounds was confirmed by SEM (Fig. 3). Some of the clusters are loose, while others consist of densely packed primary particles. The clusters were observed at concentrations as low as 1 vol% of the surface treated filler

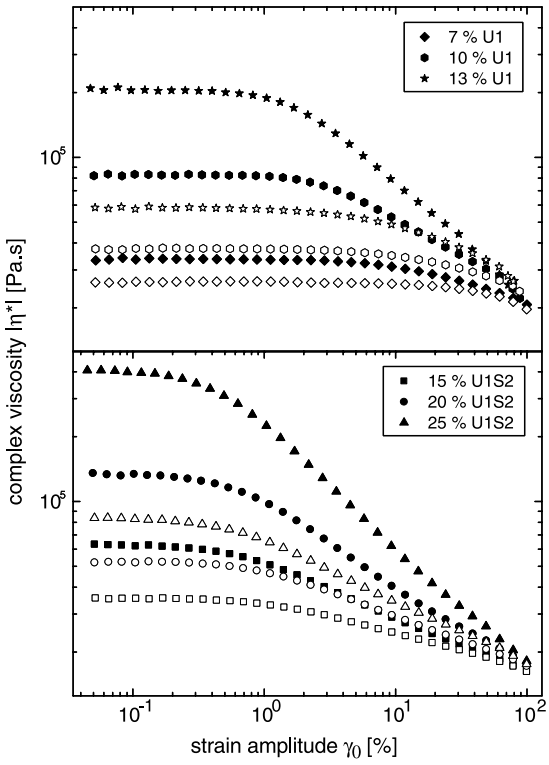

Fig. 2. Complex viscosity of $CaCO_3$–HDPE nanocomposites (treated and untreated filler) as a function of the strain amplitude at 170 °C ($\omega=1$ rad/s). Full symbols represent the first amplitude sweep, while open symbols stand for the second run after a relaxation period.

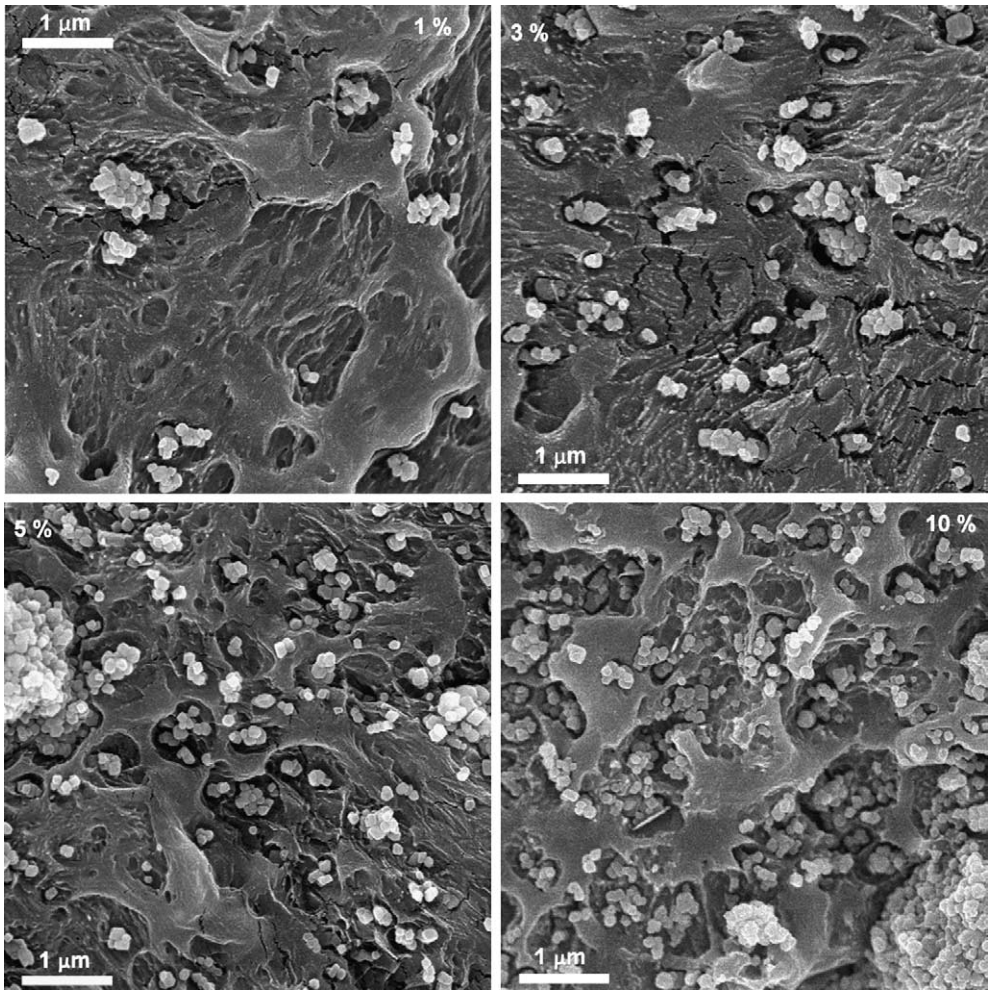

Fig. 3. SEM micrographs of the surface treated colloidal $CaCO_3$ (U1S2)–HDPE composites, 1–10 vol%.

(U1S2) and their number increased with increasing ϕ. The number of agglomerates was higher in the untreated filler (U1) composites than in those of the U1S2.

The complex viscosity of the nanocomposites as a function of γ_0 (1st and 2nd run) is compared to that of the microcomposites at different filler loading in Fig. 4. Since the AS was carried out with $\omega = 1$ rad/s, the shear rate amplitude ($\dot{\gamma}_0$) is the same in magnitude as the strain amplitude (absolute value) and the $|\eta^*| - \dot{\gamma}_0$ plots look similar to the $|\eta^*| - \gamma_0$ plots shown in Fig. 4. $|\eta^*|$ of the U1 composites is generally higher than that of the corresponding VP composites even in the second run due to the presence of clusters (aggregates) that could not be disintegrated during the first AS. $|\eta_0^*|$ of the treated and untreated VP composites was practically the same in the second run up to 25 vol% loading, suggesting the absence of agglomerates, whereas in the nanocomposites a difference can be already seen at 5 vol% loading, indicating the presence of aggregates that could not be disintegrated. The difference between the two types of composites also increases with increasing ϕ and becomes substantial at 10 vol% filler loading. The reduction in $|\eta_0^*|$ due to shearing (1st–2nd) becomes larger with increasing ϕ due to the disintegration of a larger number of agglomerates. The same behavior is observed in the composites of the surface treated filler but on a smaller scale, indicating that the surface treatment reduces the number of agglomerates. To visualize these effects, the difference in the relative zero complex viscosity between the two runs is plotted in Fig. 5 as a function of the filler volume fraction at 170 °C (ϕ is smaller than at RT due to the decrease in polymer density across the melting point). For the micron-sized filler composites the reduction in η_r^* on shearing is marginal at low filler loading, slowly increases with augmenting ϕ and becomes noticeable above 20 vol%. The effect of filler surface treatment is only substantial in the 30 vol% composite, which indicates the presence of some agglomerates. In contrast, the reduction in η_r^* of the nanocomposites due to filler surface treatment is already substantial at 7% loading and a remarkable effect can be seen at 10 vol%. The difference between the two runs increases much faster with augmenting ϕ in the nanocomposites than in the microcomposites, indicating a stronger tendency to agglomeration. The effect of shearing is more pronounced in the U1 composites in accordance with the known tendency of non-treated fillers to build clusters. Therefore, the high viscosity of the nanocomposites is not a direct consequence of the particle size but can be attributed to the strong tendency of small particles to agglomerate and

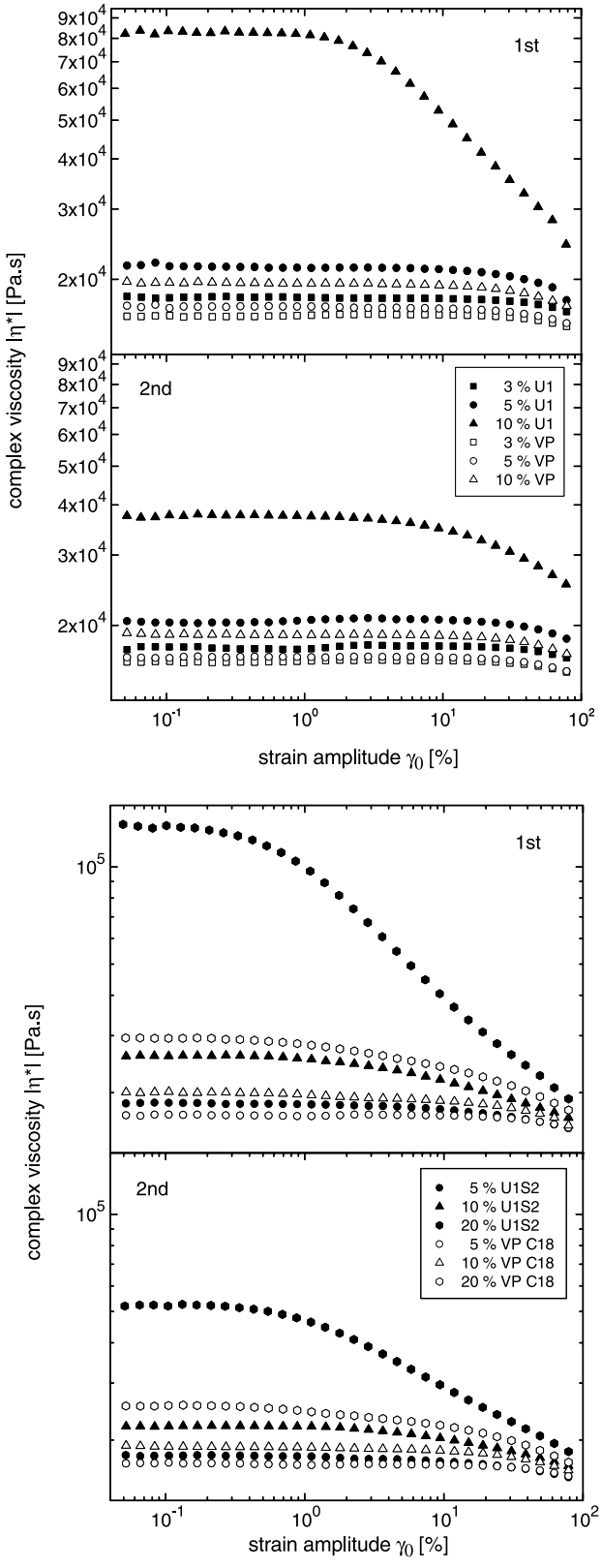

Fig. 4. Comparison between the complex viscosity of $CaCO_3$–HDPE nanocomposites (treated and untreated filler) and that of the corresponding microcomposites (VP) as a function of the strain amplitude at 170 °C (ω= 1 rad/s). Full symbols represent the first AS, while open symbols stand for the second run after a relaxation period.

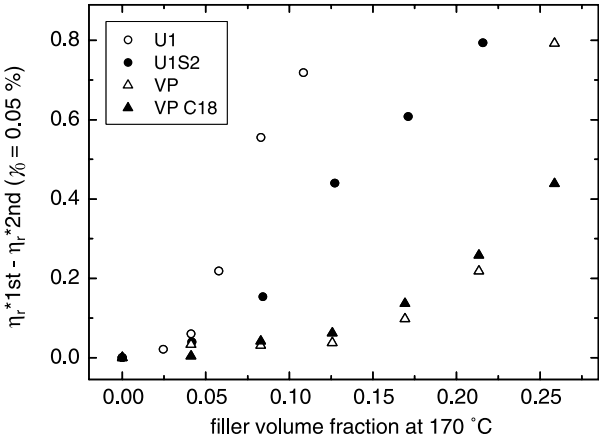

Fig. 5. Comparison between the differences in relative shear complex viscosity of treated and untreated calcite–HDPE micro- and nanocomposites measured in the 1st and 2nd amplitude sweeps at γ_0=0.05% (ω=1 rad/s) as a function of the filler volume fraction at 170 °C.

aggregate. The higher number and strength of the clusters in the nanocomposites compared to the microcomposites can be explained by the enhanced interparticle attraction, resulting from the enormous increase in specific surface area with decreasing particle size. The strength, size and number of the clusters depend on the attraction forces and contact area between the particles, which is a function of their SSA and geometry. The volume specific surface area (VSSA) of cubic and spherical particles with a specific gravity of 2.7 g/mL (calcite) is plotted as a function of the particle diameter in Fig. 6. As can be seen, the VSSA tremendously increases with decreasing diameter below 600 nm.

The filler surface treatment did not only reduce $|\eta_0^*|$ (due to less agglomeration) but also led to stronger shear thinning (Figs. 2 and 4). A comparison of the curves of the treated and untreated filler composites in the 2nd run, where no more thinning due to agglomerate disintegration occurs, clearly shows this effect. The additional thinning can be attributed to interfacial slippage that occurs due to the decreased particle-matrix interactions [4,39,41,42]. With increasing SSA of the particles as well as with increasing ϕ, the interfacial slippage

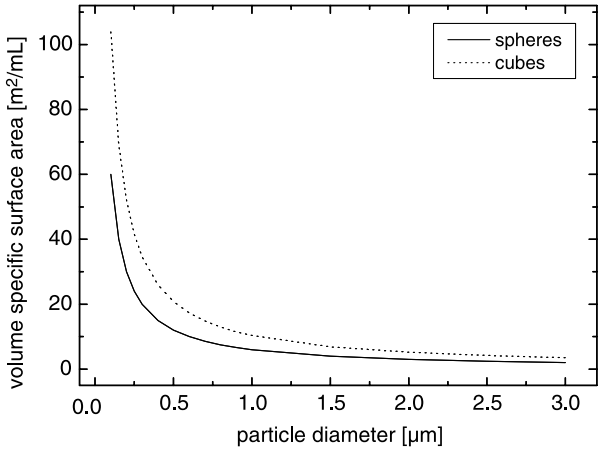

Fig. 6. Calculated volume specific surface area (VSSA) plotted as a function of the particle diameter of cubic or spherical calcite particles.

became more pronounced, leading to stronger shear thinning (Fig. 4). The viscoelastic linear regime in the treated filler composites was also generally smaller than in those of the untreated filler and was not broadened by the shearing in the first AS, supporting the notion that interfacial slippage occurs in the treated filler composites.

Plots of the storage (G') and loss (G'') moduli of the composites as functions of γ_0 also showed a linear region followed by a nonlinear one. The slope of the nonlinear part increased and the linear range decreased with increasing filler volume fraction. Both moduli increased in magnitude with rising ϕ but the increase in G' was larger than in G''. This behavior reflects the reinforcing effect of the inclusions (primary particles and clusters) and the change in the microstructure of the composites with increasing shear rate. To visualize these effects, the relative (composite/HDPE) moduli G'_r and G''_r at $\gamma_0 = 0.05$ (linear) and 49% (nonlinear) are plotted as functions of ϕ in Fig. 7 (different *Y*-scales). At large strain amplitude, i.e. after agglomerate disintegration, G'_r of the U1 composites is practically the same in both runs (1st and 2nd) and the filler surface treatment reduces its value. However, at low strain amplitude, G'_r of the untreated filler nanocomposites enormously increases with rising ϕ in the first run, showing the strong effect of clusters on the polymer elasticity. This contribution is reduced in the U1S2 composites in line with the fact that the filler surface treatment reduces the tendency to agglomeration. In the 2nd run, the $G'_r - \phi$ dependency is smaller and the values become lower with the filler surface treatment, confirming the effect of the clusters on G'. This behavior is similar to that observed in the microcomposites, however, on a larger scale, indicating intense agglomeration [4]. For example, at $\gamma_0 = 49\%$ G'_r of the 13% U1 nanocomposite is similar to that of the 25% VP microcomposite. G'_r of the U1 composites 2nd run at $\gamma_0 = 0.05\%$ started to appreciably differ from that measured in the 1st run at 7% loading, whereas a similar difference between the two runs could only be observed at 25% VP and the value of G'_r at $\phi = 13\%$ U1 is even higher than that of the 30% microcomposite. The nanocomposites of U1S2 showed similar correlations and differences to the composites of the treated micron-sized filler. Fig. 7 also shows that G''_r behaves similar to G'_r; however, the latter increases faster with increasing ϕ. In the 1st run at $\gamma_0 = 0.05\%$, G'_r of the nanocomposites is generally 5–10 times higher than G''_r, whereas in the 2nd run the values are similar, showing that clusters have more influence on G'. The relative loss moduli of the nanocomposites also showed the same differences to those of the microcomposites as in G'_r.

In small-amplitude oscillatory shear, $|\eta^*|$ of the neat polymer showed a nonlinear dependence on ω as expected and there was no difference between the 1st and the 2nd run (Fig. 8). The complex viscosity of the nanocomposites with low filler loading (3 and 5 vol% U1, 5 and 10 vol% U1S2) showed a ω-dependence similar to that of HDPE and there was only little difference between the two runs (AS in between). At higher filler loading, $|\eta^*|$ disproportionately increased, especially at low frequencies. $|\eta^*|$ of the high loaded

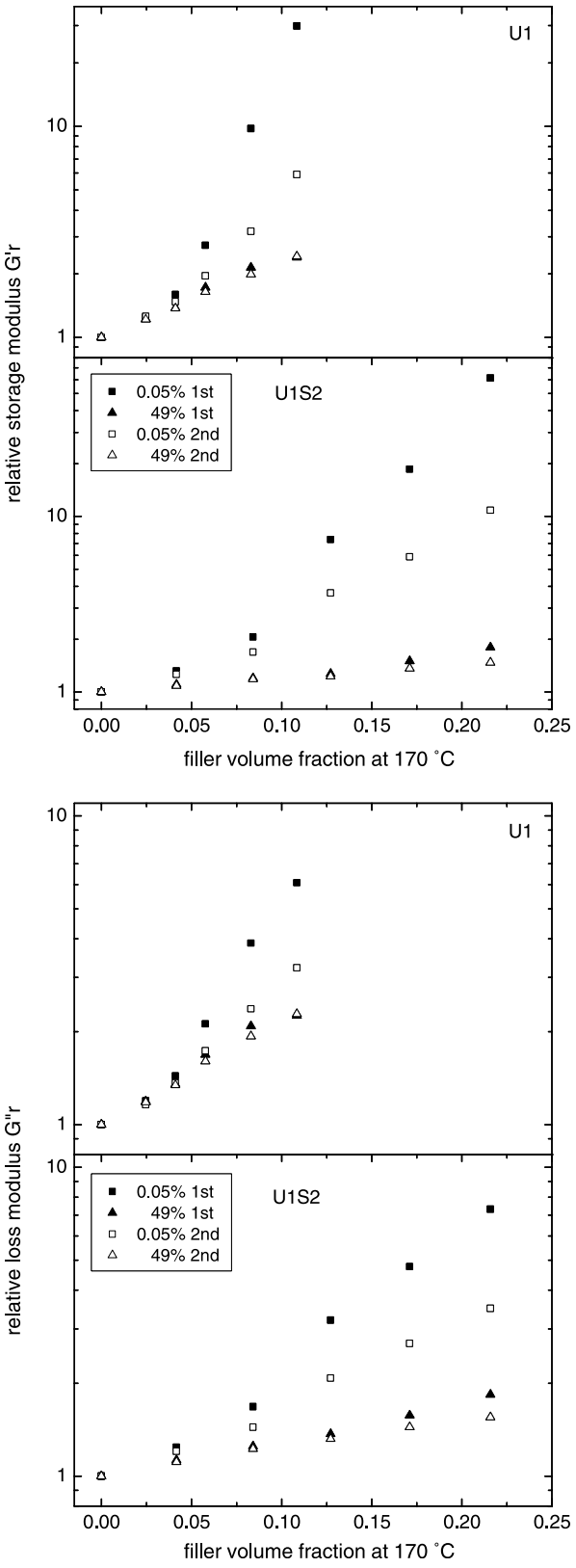

Fig. 7. Relative storage and loss moduli of treated and untreated $CaCO_3$–HDPE nanocomposites (U1 and U1S2) at $\gamma_0 = 0.05$ and 49% ($\omega = 1$ rad/s) as a function of filler volume fraction at 170 °C, 1st stands for the first AS and 2nd for the second run after a relaxation period.

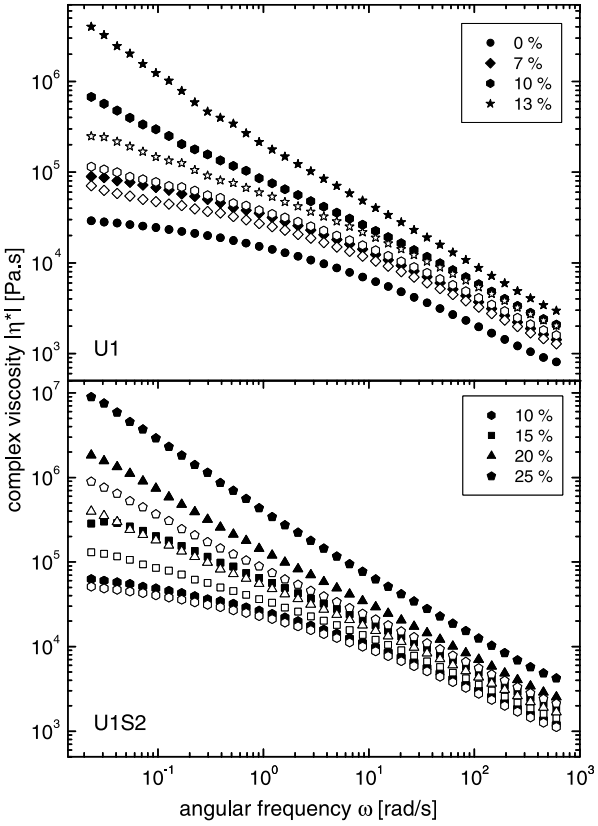

Fig. 8. Complex viscosity of $CaCO_3$–HDPE nanocomposites (treated U1S2 and untreated U1 filler) as a function of the angular frequency at 170 °C ($\gamma_0 = 0.05\%$). Full symbols represent the first run on a virgin sample, while open symbols stand for the second measurement after an amplitude sweep followed by a relaxation period.

composites, where a large number of clusters exist, diverged at low ω, showing that the effect of clusters on the viscosity is larger than that of the primary particles. The divergence seen in the viscosity curves (1st run) of the high loaded composites was reduced by shearing but did not completely disappear. The difference between the 1st and 2nd run also increased with augmenting filler loading as a result of the presence of clusters and their partial disintegration. The filler surface treatment decreased the viscosity of the composites and the difference between the two runs was smaller due to better dispersion of the filler particles, i.e. presence of less clusters. In spite of the similarity between the curves of Fig. 8 and steady shear flow curves (η–stress), there is a distinct difference between the two in that $|\eta^*|(\omega)$ is reversible, while the others are not. This is because the stress amplitude (<600 Pa) exerted on the sample in small-amplitude oscillatory experiments is small and does not significantly deform the microstructure of the complex fluid, whereas in steady shear or in AS the stress is an order of magnitude larger (up to 25′000 Pa) and the microstructure is irreversibly deformed (agglomerate disintegration). In contrast to the nanocomposites, no divergence in the low frequency zone was observed in $|\eta^*|(\omega)$ of the 20 and 25% microcomposites and only a slight divergence could be seen at 30 vol% loading, which disappeared on shearing (AS) [4]. The difference between the viscosity curves in the two runs was also much smaller in the microcomposites. This behavior can be attributed to the presence of more agglomerates and aggregates in the nanocomposites and the observed viscosity reduction in the 2nd run is a result of partial disintegration of the clusters (aggregates were not disintegrated) in the intermediate AS. Therefore, the high viscosity of the nanocomposites is not a direct consequence of the particles size but is due to the strong tendency of nanoparticles to build clusters (local structures). The presence of clusters that have different shapes and maximum packing than the nearly spherical primary particles leads to higher composite viscosity [31,43,44]. The interfacial slippage, which was seen in Fig. 4 could not be observed in the $|\eta^*|(\omega)$ curves of the treated filler composites (Fig. 8) due to the fact that the strain and the shear rates in the FS are small.

Since small-amplitude oscillatory shear does not significantly deform the microstructure of the complex fluid, it allows studying the reinforcing effect of the inclusions. The linear storage and loss moduli of the treated and untreated filler nanocomposites are shown in Fig. 9 as a function of the angular frequency. At low loading, both moduli of the non-treated filler composites increase with increasing ω and in the low frequency region G'' is larger than G', demonstrating the viscous nature of the compounds. However, the slope of $G''(\omega)$ is smaller than that of $G'(\omega)$, so that with increasing ω the two curves cross each other at ω_c (cross-over frequency). This characteristic frequency ($G' = G''$) marks a transition from viscous ($G'' > G'$) to rubbery ($G' > G''$) response. With increasing ϕ, the moduli increase over the whole frequency range but the increase is more pronounced in the low frequency region and in G' more than in G'', and the slope of $G'(\omega)$ and $G''(\omega)$ in the terminal zone of the log–log plot gradually decreases. Consequently, ω_c is shifted to lower values, indicating an increase in relaxation time (ω_c is approximately equal to the inverse of the fluid's characteristic relaxation time λ_c, roughly the longest relaxation time). It seems that the inclusions contribute to the elasticity of the complex fluid and represent topological restraints to the reptation of the polymer chains, leading to more chain stiffness and energy dissipation. Above a certain particle volume fraction, G' becomes larger than G'' over the whole measured frequency range and the two curves just come near to each other in a certain ω-range, i.e. no ω_c is observed, and the sample can be described as a viscoelastic solid. Above that concentration, both G' and G'' become almost frequency independent (log–log plot) in the low frequency region. Generally, frequency-independent moduli are characteristic for solids and indicate here that the polymer relaxation is quite slow and the chain reptation is strongly restrained. Such terminal plateaus were not observed in the microcomposites up to 30% loading [4]. In the 2nd run, the slope of $G'(\omega)$ and $G''(\omega)$ in the terminal zone of the log–log plot is larger than in the first run and the terminal plateau disappears, showing a correlation between the presence of clusters and the low-frequency plateau. The nanocomposites of the treated filler show a similar behavior in both runs (1st and 2nd); however, the filler volume fraction, above which

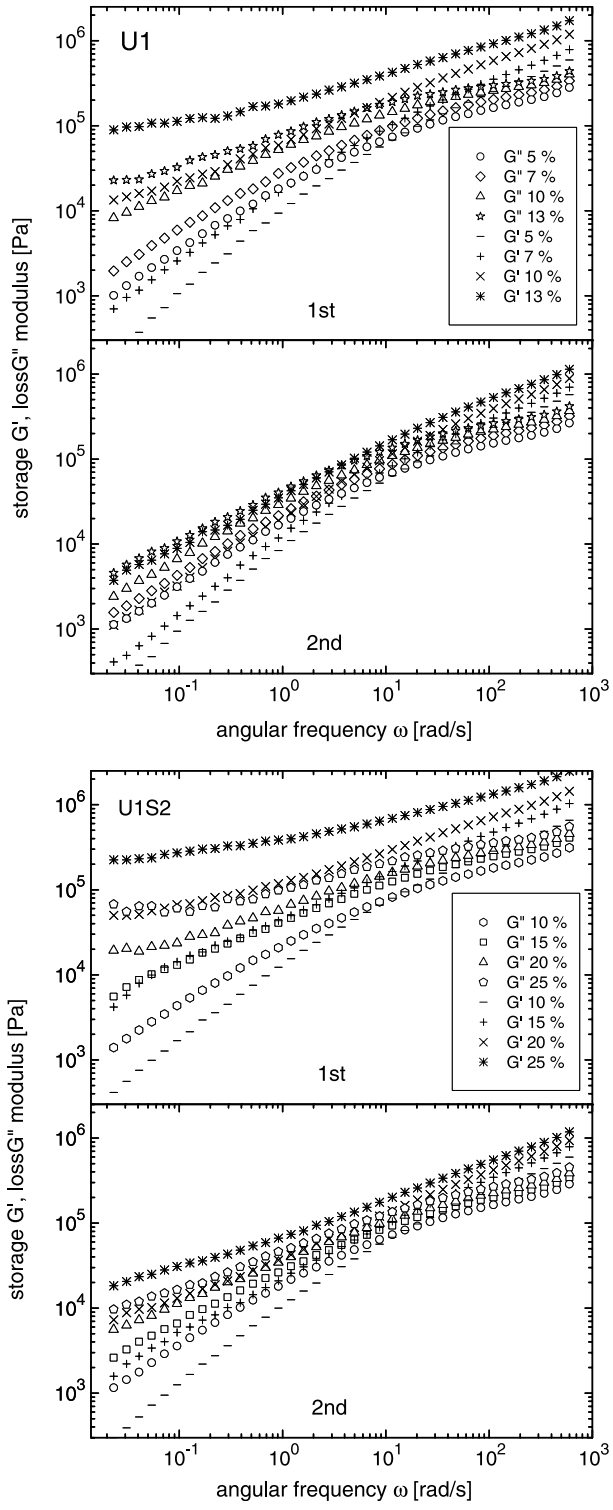

Fig. 9. Storage and loss moduli of treated (U1S2) and untreated (U1) $CaCO_3$–HDPE nanocomposites plotted as a function of the angular frequency at 170 °C ($\gamma_0 = 0.05\%$), 1st stands for the first FS and 2nd for the second run after an AS and a relaxation period.

the composites respond as a viscoelastic solid, increases with the filler surface treatment. This filler volume fraction is 10% for U1 and increases to >13% in the 2nd run; is 20% for U1S2 and increases to 25% in the 2nd run.

To visualize the change in the moduli dependence on ω with increasing ϕ as well as with filler surface treatment, the slope of $\log G'(\log \omega)$ and $\log G''(\log \omega)$ in the range $\omega =$ 0.02–0.07 rad/s (lowest frequency range measured) is plotted as a function of ϕ in Fig. 10. In the first run, the slope of both moduli of the untreated filler nanocomposites sharply decreases with augmenting ϕ to become almost ω-independent (slope $\log G'(\log \omega) < 0.4$) at 10 vol%. In the second run, the decrease in slope is slower and the moduli remain frequency dependent at the highest filler concentration. The decrease in slope of the moduli is also less pronounced in the treated nano-filler composites and ω-independence is nearly reached at 20 vol%. It is to be noted that the weak ω-dependence corresponds well with the divergence of the $|\eta^*|(\omega)$ curves in Fig. 8. These results show that local structures (clusters), depending on their number and strength (a consequence of the interparticle and particle–matrix interactions), lead to a gradual increase in moduli and decrease in their ω-dependency. The moduli dependence on ω in the microcomposites is similar to that of the nanocomposites (Fig. 10) and ω_c is shifted to lower values with increasing ϕ [4]. Both moduli increase with increasing ϕ but not as fast as in the nanocomposites and no viscoelastic solid rheological response was observed in these composites up to 30% filler loading. As can be seen in Fig. 10, the slope of $\log G'(\log \omega)$ and $\log G''(\log \omega)$ of the microcomposites decreases with increasing ϕ, and the decrease is shear and filler surface treatment dependent. The decrease is also not as sharp as in the nanocomposites and the moduli remain ω-dependent up to 30% loading ($\log G'(\log \omega)$ slope < 0.4 is not reached). This is in accordance with the fact that filler clusters are fewer and weaker in the microcomposites than in the nanocomposites. The primary particles of both colloidal and non-colloidal fillers are nearly spherical and have the same geometrical percolation threshold. That is, the critical volume fraction ϕ_c, at which a space-filling network is built, should be the same. However, clusters have different shapes and maximum packing that can lead to lower ϕ_c. In both micro- and nanocomposites, the moduli gradually increase and the slope of $\log G'(\log \omega)$ and $\log G''(\log \omega)$ gradually decreases with increasing number of clusters. It is difficult to determine whether ϕ_c has been reached or not, since no abrupt change occurs.

The loss factor $\tan \delta$ (G''/G') of the nanocomposites measured in small-amplitude oscillatory shear is given in Fig. 11 as a function of ω. At low filler loading, $\tan \delta$ is high and decays very fast with increasing ω similar to that of the polymer matrix to reach a value ≤ 0.5. With increasing ϕ, $\tan \delta$ decreases and its decay rate diminishes as well, so that the curves become almost flat, i.e. show a very broad peak (arc), reflecting the development of clusters with increasing ϕ and their influence on the moduli. In the 1st run, the U1 composites show such behavior at $\phi \geq 10\%$ and $\tan \delta$ is <1 ($G' > G''$), while in the 2nd run this behavior is only observed in the 13% composite. In the U1S2 composites, $\tan \delta$ starts to be almost ω-independent and is <1 at $\geq 20\%$, indicating a solid-like behavior. The magnitude of $\tan \delta$ is always lower in

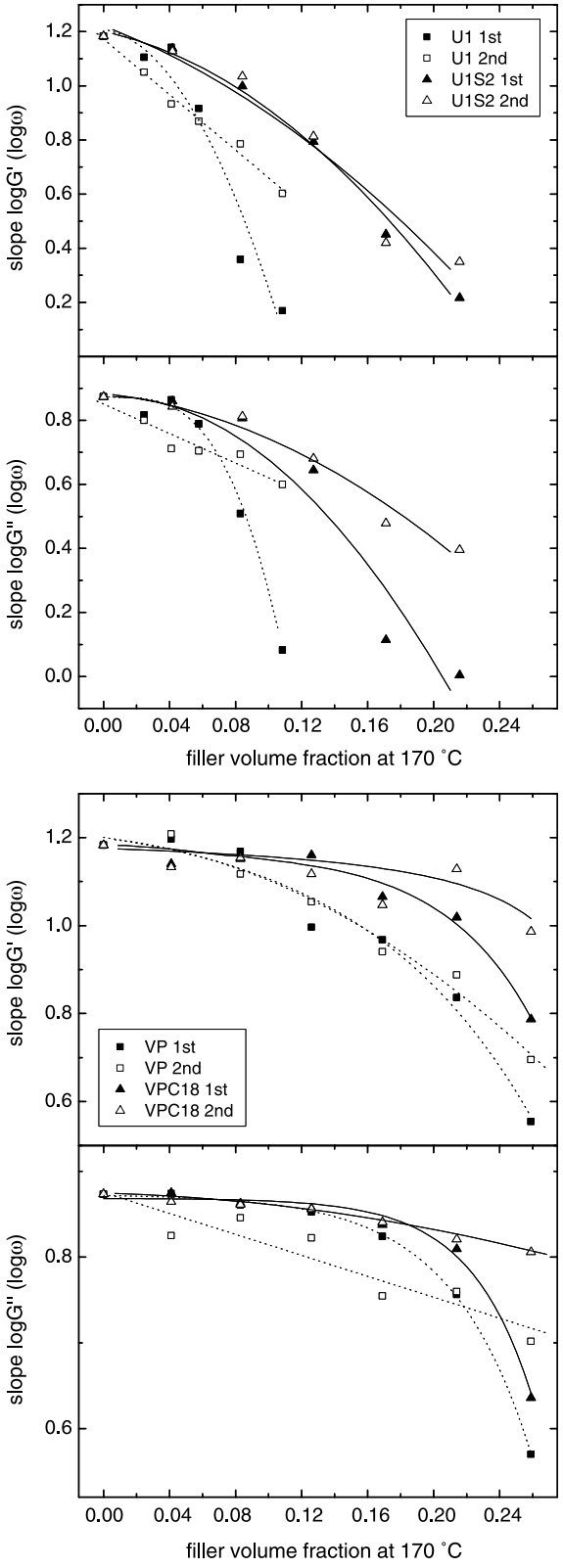

Fig. 10. Change in slope of log $G'(\log \omega)$ and log $G''(\log \omega)$ in the range $\omega = 0.02$–0.07 rad/s of $CaCO_3$–HDPE nano- and microcomposites with increasing volume fraction of treated and untreated filler.

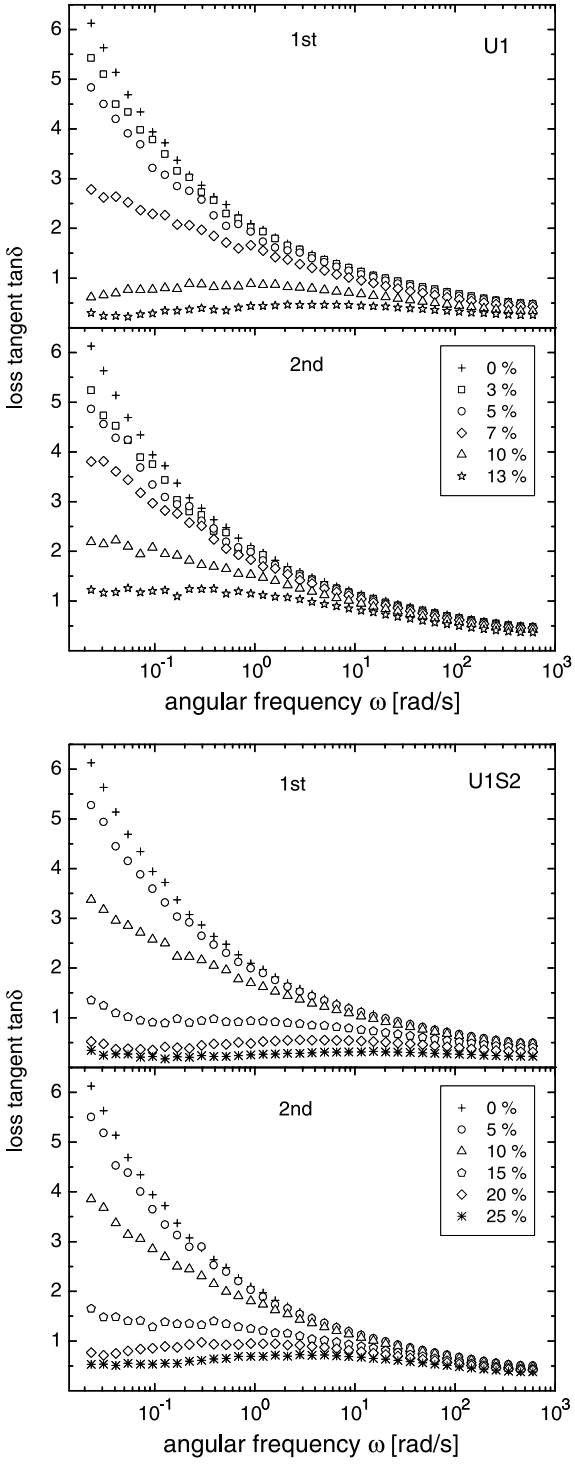

Fig. 11. Loss factor tan δ plotted as a function of the angular frequency for treated (U1S2) and untreated (U1) $CaCO_3$–HDPE nanocomposites, 1st stands for the first FS and 2nd for the second run after an AS and a relaxation period.

the 1st run than in the 2nd and in the untreated filler composites than in those of the treated one. This behavior is similar to that observed in the microcomposites, except for the fact that in those composites only a weak frequency-dependence was indicated at 30 vol% untreated filler and disappeared on preshearing and on filler surface treatment [4].

These results confirm that the presence of clusters, whose number and strength is determined by the SSA of the filler, shearing and surface treatment of the filler, increases G' (storage of elastic energy) more than G'' (viscous dissipation of that energy) of the composites.

The effect of the inclusions (primary particles and clusters) on the moduli of the nanocomposites is ostensive seen in the linear relative (composite/matrix) storage G'_r and loss moduli G''_r-angular frequency plots (Fig. 12). The relative moduli of the nanocomposites are ω-dependent in the low frequency region and gradually increase with augmenting filler loading. The ω-dependency decreases with increasing frequency, preshearing, filler surface treatment and decreasing ϕ so that the relative moduli become ω-independent over the whole frequency range in the 5 vol% U1S2 composite. The ω-independent contribution to the moduli at high frequencies represents the instantaneous hydrodynamic reinforcement by the inclusions [4]. A similar observation was made in the microcomposites, though the relative moduli were an order of magnitude lower [4]. Since the composite microstructure is not significantly deformed during the FS, the relative modulus decay with increasing frequency cannot be attributed to de-agglomeration of filler clusters. Cluster disintegration in a highly viscous polymer melt (hindered Brownian motion) is also an irreversible process, while the relative moduli decay with increasing ω is a reversible one. The additional contribution to the moduli at low ω, which must be due to slow relaxation processes can, therefore, be attributed to polymer adsorption on the filler surface. The polymer adsorption provides additional localized junctions, leading to a transient polymer–filler network. The dynamics of the bound polymer is also expected to be different from that of the bulk; however, it is difficult to distinguish the contribution of a transient network from that of retarded chain dynamics. The relative moduli are smaller after preshearing (2nd run) and after surface treatment of the filler (Fig. 12). The disproportionate increase in relative moduli with increasing ϕ can therefore be attributed to the presence of augmenting number of clusters. A comparison between the relative moduli of the nanocomposites and those of the corresponding microcomposites reveals an increase, which by far exceeds the increase in specific surface area of the filler particles [4]. In contrast to the microcomposites, a large number of aggregates, which cannot be disintegrated by shear in the AS, are present in the nanocomposites, leading to higher moduli. That is, the low frequency contribution to the moduli has two components; one is coming from polymer adsorption and the other is due to the presence of clusters. Clusters assume shapes that are different from that of the nearly spherical primary particles and exert larger topological restraints on the polymer relaxation.

Figs. 13 and 14 compare the evolution of G'_r and G''_r of the micro- and nanocomposites with increasing ϕ at two different frequencies, 0.031 and 453 rad/s, and show the effect of preshearing and filler surface treatment on the relative moduli. It can be seen that:

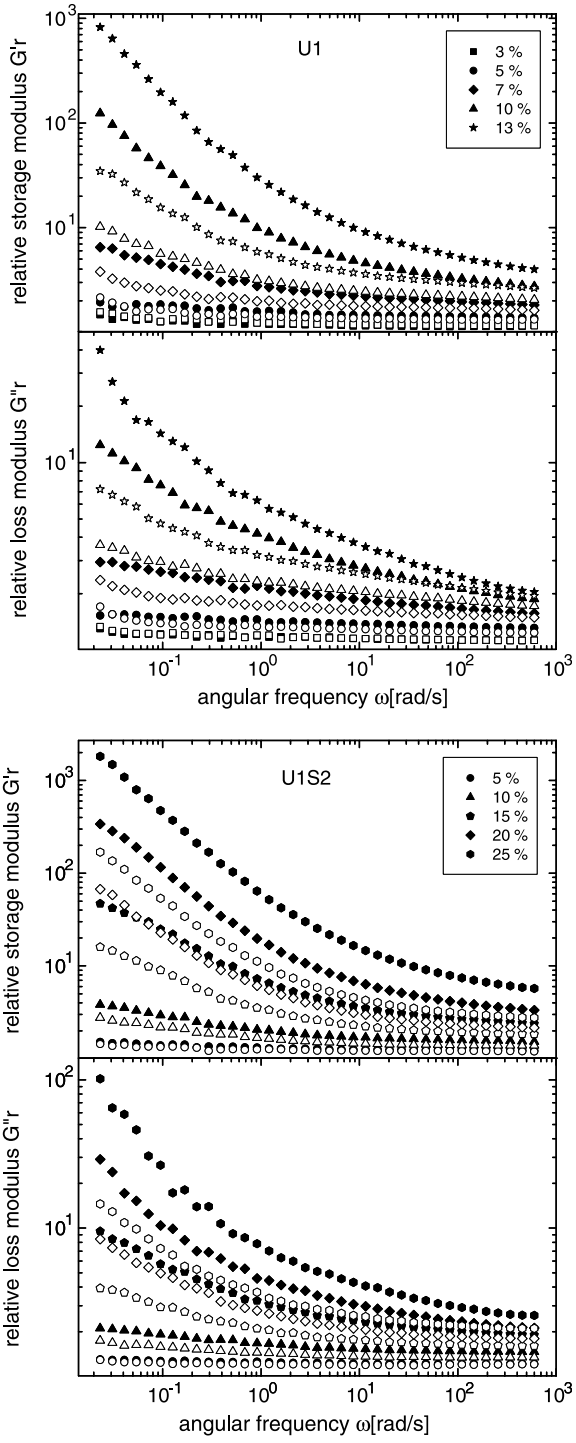

Fig. 12. Relative storage and loss moduli of treated (U1S2) and untreated (U1) $CaCO_3$–HDPE nanocomposites plotted as a function of the angular frequency ($\gamma_0 = 0.05\%$) at 170 °C. Full symbols represent the first run on a virgin sample, whereas open symbols stand for the second measurement after an amplitude sweep followed by a relaxation period.

- In all cases, G'_r and G''_r are nonlinear functions of ϕ.
- Both relative moduli become lower after preshearing or filler surface treatment.
- At the high frequency, the moduli dependence on ϕ is smaller than at the low frequency and becomes also smaller due to filler surface treatment.

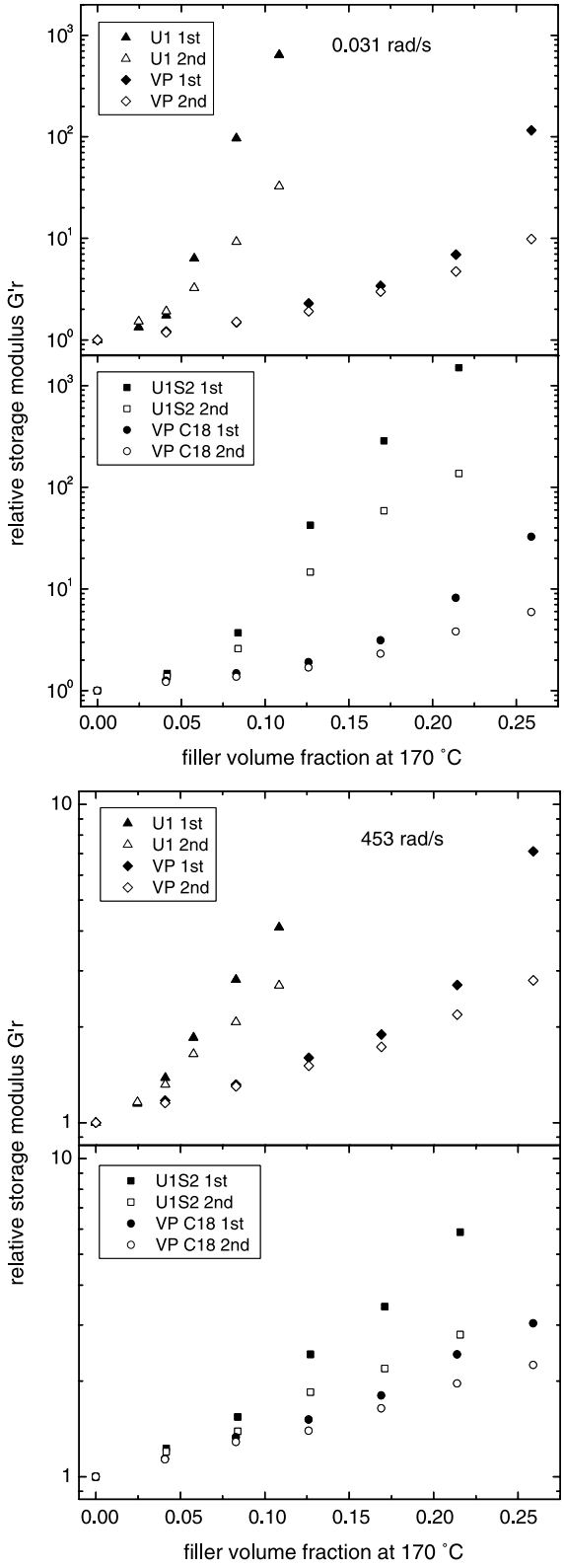

Fig. 13. Relative storage modulus of treated and untreated $CaCO_3$–HDPE composites at $\omega=0.031$ and 453 ($\gamma_0=0.05\%$) as a function of filler volume fraction at 170 °C, 1st stands for the first FS and 2nd for the second run after an AS and a relaxation period.

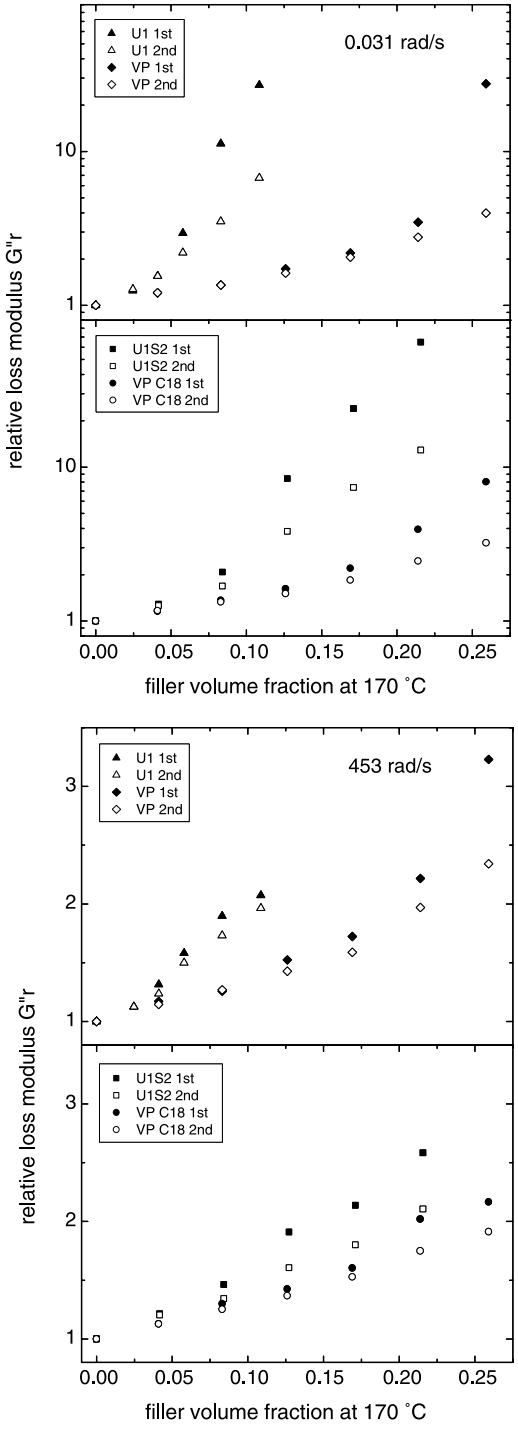

Fig. 14. Relative loss modulus of treated and untreated $CaCO_3$–HDPE composites at $\omega=0.031$ and 453 ($\gamma_0=0.05\%$) as a function of filler volume fraction at 170 °C, 1st stands for the first FS and 2nd for the second run after an AS and a relaxation period.

- At the low frequency, G'_r and G''_r of the nanocomposites are much larger than those of the microcomposites, whereas at the high frequency they are of the same order of magnitude (nanocomposites still higher).
- At the low frequency, G'_r of the nanocomposites is generally an order of magnitude larger than G''_r, while in the

microcomposites it is only 2–4 times larger. At the high frequency, G'_r is only slightly larger than G''_r.

These results indicate that solid spherical (primary) particles offer different contributions to the composite's moduli due to their influence on the hydrodynamics and the relaxation of the polymer melt. The instantaneous hydrodynamic contribution is observed at high frequencies, while in the terminal zone the sum of all contributions is measured. Polymer adsorption on the particles' surface leads to slow chain dynamics and transient filler–polymer network. This leads to the slow polymer relaxation is observed in the low frequency region. Clusters exert stronger restraints on the polymer relaxation than the nearly spherical primary particles. These local structures have different shapes and maximum packing, therefore provide an additional disproportionate contribution to the moduli long before ϕ_c is reached.

4. Conclusions

Submicron-sized particles have strong tendency to build agglomerates and aggregates due to their high specific surface area. The number and strength of the clusters are higher in polymer nanocomposites than in the microcomposites and are functions of the filler volume fraction. The clusters (local structure) strongly increase the moduli and viscosity of the composites, especially at low frequencies. They enhance G' more than G'' and decrease the slope of $\log G'(\log \omega)$ and $\log G''(\log \omega)$ in the terminal region. Polymer adsorption on the particles' surface results in a transient filler–polymer network and slow dynamics of the bound polymer, which contribute to the moduli of the complex fluid. Above a certain filler volume fraction, the composite responds as a viscoelastic solid as a result of the different reinforcing contributions. Consequently, the terminal plateau is not necessarily an evidence for the presence a space-filling filler network. The high moduli and viscosity of the nanocomposites is not a direct consequence of the particle size but is due to the presence of a large number of agglomerates and aggregates in these composites.

Acknowledgements

We gratefully acknowledge financial support from the Swiss National Science Foundation (SNF).

References

[1] Katz HS, Milewski JV, editors. Hand book of fillers for plastics. New York: Van Nostrand Reinhold Company; 1987.
[2] Rothon RN, editor. Particulate-filled polymer composites. Harlow: Longman Scientific and Technical; 1995.
[3] Osman MA, Suter UW. Chem Mater 2002;14:4408.
[4] Osman MA, Atallah A. Polymer 2005;46:9476.
[5] Barnes HA, Hutton JF, Walters K. An introduction to rheology. Amsterdam: Elsevier; 1989.
[6] Larson RG. The structure and rheology of complex fluids. New York: Oxford University Press; 1999.
[7] Halpin JC. Primer on composite materials analysis. Lancaster: Technomic Publishing Company: 1992
[8] Nielsen LE, Landel RF. Mechanical properties of polymers and composites. New York: Marcel Dekker; 1994.
[9] Choi GN, Krieger IM. J Colloid Interface Sci 1986;113:101.
[10] Vollenberg PHT, Heikens D. Polymer 1989;30:1656.
[11] Cai JJ, Salovey R. Polym Eng Sci 1999;39:1696.
[12] Van der Werff JC, de Kruif CG. J Rheol 1989;33:421.
[13] Suetsugu Y, White JL. J Appl Polym Sci 1983;28:1481.
[14] Li L, Masuda T. Polym Eng Sci 1990;30:841.
[15] Le Meins JF, Moldenaers P, Mewis J. Ind Eng Chem Res 2002;41:6297.
[16] Poslinski AJ, Rayan ME, Gupta RK, Seshadri SG, Frechette FJ. J Rheol 1988;32:703.
[17] Lobe VM, White JL. Polym Eng Sci 1979;19:617.
[18] Gandhi K, Salovey R. Polym Eng Sci 1988;28:877.
[19] Sun L, Park M, Salovey R, Aklonis JJ. Polym Eng Sci 1992;32:777.
[20] Agarwal S, Salovey R. Polym Eng Sci 1995;35:1241.
[21] Wang Y, Wang JJ. Polym Eng Sci 1999;39:190.
[22] Wang Y, Yu MJ. Polym Compos 2000;21:1.
[23] Malik TM, Carreau PJ, Germela M, Dufresne A. Polym Compos 1988;9:412.
[24] Schaefer DW, Martin JE, Wiltzius P, Cannell DS. Phys Rev Lett 1984;52:2371.
[25] Eggers H, Schümmer P. Rubber Chem Technol 1996;69:253.
[26] Yziquel F, Carreau PJ, Tanguy PA. Rheol Acta 1999;38:14.
[27] Yurekli K, Krishnamoorti R, Tse MF, Mcelrath KO, Tsou AH, Wang HC. J Polym Sci, Part B: Polym Phys 2001;39:256.
[28] Trappe V, Weitz DA. Phys Rev Lett 2000;85:449.
[29] Paquien JN, Galy J, Gérard JF, Pouchelon A. Colloids Surf A 2005;260:165.
[30] Rintoul MD, Torquato S. J Phys, A: Math Gen 1997;30:L585.
[31] Bicerano J, Douglas JF, Brune DA. JMS Rev Macromol Chem Phys 1999;C39(4):561.
[32] Mecke KR, Seyfried A. Europhys Lett 2002;58:28.
[33] Pishvaei M, Graillat C, McKenna TF, Cassagnau P. Polymer 2005;46:1235.
[34] Aranguren MI, Mora E, DeGroot JV, Macosko CW. J Rheol 1992;36:1165.
[35] Sternstein SS, Zhu AJ. Macromolecules 2002;35:7262.
[36] Heinrich G, Klüppel M. Adv Polym Sci 2002;160:1.
[37] Picu RC, Ozmusul MS. J Chem Phys 2003;118:11239.
[38] Vilgis TA. Polymer 2005;46:4223.
[39] Osman MA, Atallah A, Schweizer T, Öttinger HC. J Rheol 2004;48:1167.
[40] Nielsen LE. J Polym Sci, Part B: Polym Phys 1979;17:1897.
[41] Wang SQ, Inn YW. Rheol Acta 1994;33:108.
[42] Inn YW, Wang SQ. Langmuir 1995;11:1589.
[43] Jeffrey DJ, Acrivos A. AICHE J 1976;22:417.
[44] Douglas JF, Garboczi EJ. Adv Chem Phys 1995;41:85.